



## Near-Infrared OAM Communication Using 3D-Printed Microscale Spiral Phase Plates

Item Type	Article
Authors	Stegenburgs, Edgars;Bertoncini, Andrea;Trichili, Abderrahmen;Alias, Mohd Sharizal;Ng, Tien Khee;Alouini, Mohamed-Slim;Liberale, Carlo;Ooi, Boon S.
Citation	Stegenburgs, E., Bertoncini, A., Trichili, A., Alias, M. S., Ng, T. K., Alouini, M.-S., ... Ooi, B. S. (2019). Near-Infrared OAM Communication Using 3D-Printed Microscale Spiral Phase Plates. IEEE Communications Magazine, 57(8), 65–69. doi:10.1109/mcom.2019.1800902
Eprint version	Post-print
DOI	<a href="https://doi.org/10.1109/mcom.2019.1800902">10.1109/mcom.2019.1800902</a>
Publisher	Institute of Electrical and Electronics Engineers (IEEE)
Journal	IEEE Communications Magazine
Rights	(c) 2019 IEEE. Personal use of this material is permitted. Permission from IEEE must be obtained for all other users, including reprinting/ republishing this material for advertising or promotional purposes, creating new collective works for resale or redistribution to servers or lists, or reuse of any copyrighted components of this work in other works.
Download date	2023-11-29 19:43:05
Link to Item	<a href="http://hdl.handle.net/10754/656656">http://hdl.handle.net/10754/656656</a>

# Near-Infrared OAM Communication Using 3D-Printed Microscale Spiral Phase Plates

Edgars Stegenburgs, Andrea Bertoncini, Abderrahmen Trichili, Mohd Sharizal Alias, Tien Khee Ng, Mohamed-Slim Alouini, Carlo Liberale, and Boon S. Ooi

## ABSTRACT

We report the use of 3D-printed microscale spiral phase plates to generate orbital angular momentum (OAM) carrying beams. We confirm that the generated beams have high purity, and we have successfully tested them to convey data signals with low bit error rates at the wavelength of 980 nm. This method will open new opportunities for generating OAM beams for many applications in optical communications, including free-space optics, as well as underwater, chip-to-chip, and quantum communications.

## INTRODUCTION

SINCE their initial discovery by Allen *et al.* in the 1990s, orbital angular momentum (OAM) beams have been used in imaging, quantum optics, remote sensing, optical manipulation and trapping, and so forth [1]. A light beam that carries an OAM is a beam with a helical wavefront and is characterized by an azimuth-dependent phase term  $\exp(i\ell\phi)$ , where the topological charge  $\ell$  (also known as the azimuthal mode index) can have any integer value [2]. A noticeable difference between the “orbital” angular momentum and the “spin” angular momentum, which is related to circular polarization, is that the latter has only two states: “right-handed” and “left-handed,” while the former gives access to an infinite number of states. Two OAM beams with distinct azimuthal mode indices are orthogonal to one another. This characteristic has attracted considerable attention for the use of OAM multiplexed light beams to convey independent data streams, which scale the transmission capacity of the optical communication systems by several orders of magnitude. The OAM is considered a mode of choice of spatial-division multiplexing (SDM) proposed as a solution to address future bandwidth issues and ease the upcoming “capacity crunch” [3, 4]. OAM multiplexing can be combined with other multiplexing schemes that involve the use of multiple wavelengths and orthogonal polarization states. Mapping the data carried by each OAM beam can be additionally done using high-order modulation formats such as quadrature phase shift keying (QPSK) and M-ary quadrature amplitude modulation (M-QAM). OAM multiplexing enables transmission capacities beyond terabit per second and communication links with very high spectral efficiency values over free-space channels and optical fibers [5, 6]. Fast on-chip-scale OAM free-space interconnections were also recently reported [7].

Extensive works have been done on the generation of OAM communication degree of freedom. Different technologies are

realized to twist the wavefront of Gaussian beams from laser sources to generate OAM light, including spiral phase plates (SPPs), q-plates, metamaterials, fiber couplers, computer-generated holograms (CGHs) programmed on spatial light modulators (SLMs), and digital micromirror devices (DMDs) [3]. Of note, most OAM generation methods are only efficient in finely aligned laboratory testbed experiments, which often are too bulky to incorporate in practical communication systems. Some existing generation techniques also suffer from low conversion efficiency, for example, the SLM where most of the incident light energy goes to an unwanted zero-order-diffracted beam [3]. Additional challenges are imposed by the requirement of a particular polarization state to fulfill the mode conversion operation, such as the case of q-plates, where only circularly polarized light beams can be converted into OAM beams. Similar polarization restrictions apply for several commercially available liquid-crystal-based SLM models, where the polarization of the incident beam should match the working polarization of the used SLM via polarizers and waveplates. Therefore, such generation methods cannot be viewed as cost-effective solutions to establish practical out-of-laboratory wireless communication links. Instead, real-world deployment of OAM-based optical communication networks requires developing laser sources with the integrated OAM generation capability [7].

Several approaches can be used to realize the OAM integration with a light source. The first approach is putting an OAM converter such as a spiral phase plate that breaks the rotational symmetry of the transverse mode directly on a laser source. Using the direct scheme, lasers such as the microchip laser [8] have been demonstrated recently. The second approach is an indirect scheme by controlling the transverse mode of the laser using optical feedback from an external cavity [9]. This approach includes the use of photonic structures in the form of a metamaterial, ring-shaped waveguide using the standard distributed Bragg reflector (DBR), and microring cavity using the azimuthal DBR or grating with whispering gallery modes. The monolithically integrated distributed feedback (DFB) semiconductor laser with a microring cavity [10], microring-based tunable OAM emitters [11], and novel structure OAM (de)multiplexers [12] have been experimentally demonstrated. The direct scheme is preferred for small footprint and device applications with a fixed OAM mode output, which enables the near-lossless generation of high-purity beams. In some cases, the indirect scheme provides the flexibility of selecting the OAM mode by controlling the topological charge and

amplitude of the generated OAM light. However, the indirect scheme involves losing a significant amount of light intensity through diffraction, scattering, and coupling losses.

In this work, we demonstrate the microscale SPPs fabricated by two-photon lithography, which can produce high-purity OAM beams that can be used as information carriers. The 3D-printed microstructured SPPs by two-photon lithography have shown very promising results [13]. This approach presents clear advantages in the fabrication of micro-optics elements, such as the flexibility, rapid prototyping, straightforward integration with photonic devices, submicrometric resolution, high throughput, and high yield. Then the performance of the fabricated SPPs to generate OAM beams that carry high-data-rate signals is tested in the near-infrared region at the wavelength of 980 nm. We demonstrate that our fabricated SPPs are a versatile tool to generate high-quality OAM beams for signal delivery purposes. These structures can be equally well integrated into photonic circuits and laser sources such as vertical-cavity surface-emitting lasers (VCSELs), which have great potential for communication and interconnection applications [7]. We note that VCSELs are semiconductor laser diodes that perpendicularly emit light to the top surface, unlike edge-emitting lasers, which emit light in parallel to the wafer surface.

### SPP DESIGN AND FABRICATION

The spiral phase plate is a simple structure that introduces a phase shift to an incoming light beam by an optical path difference that rotationally increases or decreases with the azimuth along the optical axis. The resulting beam wavefront becomes twisted or helical in space. An SPP that can produce the OAM with a topological charge of +1 is shown in Fig. 1 (first row,  $\ell = +1$ ), and it resembles a rotating staircase. An analog example is a clock with an hourly dial. We assume that the hour value reflects the phase value at the same point, which is radially constant with the dial but increases as the dial rotates until it reaches the maximum value at the 12 o'clock direction followed by an abrupt return to the initial value of zero. The number of staircases corresponds to the absolute value of the topological charge. We note that the design of the staircases should be made in accordance with the expression of the total height difference between the lowest and highest points of the helical surface:  $H = \lambda/(n - n_0)$ , where  $\lambda$  is the incident wavelength,  $n$  is the refractive index of the SPP material, and  $n_0$  is the refractive index of the medium in which the helical surface is immersed.

Designs of fabricated SPPs are shown in the first row of Fig. 1, and they consist of four different SPPs with  $|\ell|$  of 1–4. SPPs of 20 and 100  $\mu\text{m}$  diameters are fabricated on a glass substrate using a 3D direct laser writing system based on the two-photon absorption with a proprietary photoresist for high resolution. The refractive index of this photoresist was interpolated based on the results in [14], that is,  $n \approx 1.537$  at 980 nm wavelength that coincides with the laser emission and is within the SLM-supported spectral range in the current work. This material features negligible absorption in the near-infrared range; therefore, these SPPs are of low loss and

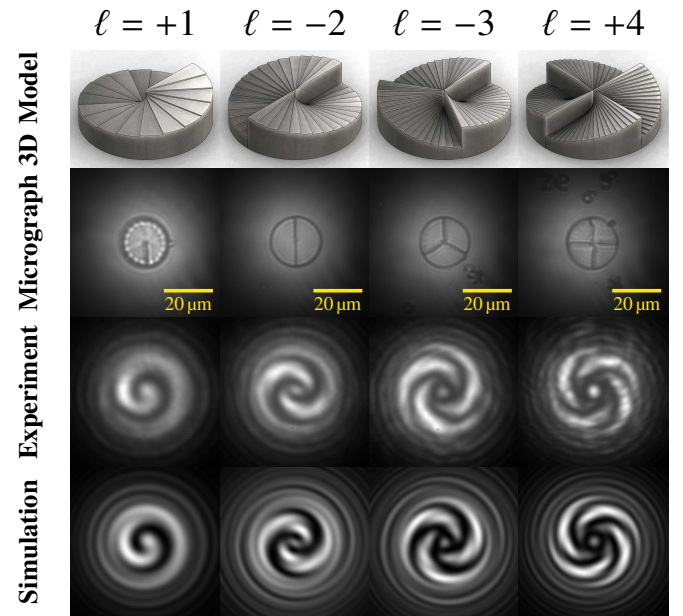


**Figure 1.** First row: 3D schematic of the fabricated SPPs; second row: a set of 20- $\mu\text{m}$ -diameter microscale SPPs printed on a glass substrate; third and fourth rows: experimental and simulated corresponding single-beam interferograms.

suitable for high-power applications. Each SPP segment (staircase) of the twisted helical surface corresponds to a  $2\pi$  phase shift and is discretized into 18 equal flat steps, so every step on each rotating staircase introduces a phase shift by the same amount of  $\pi/9$ . A set of microscale SPPs illuminated by light with a wavelength of 980 nm and the corresponding recorded single-beam interferograms are depicted in Fig. 1. This type of interference is formed when a Gaussian beam with the transverse size larger than the fabricated SPP passes through it, resulting in interference image formed by the generated OAM and the unperturbed Gaussian parts of the beam. The recorded interferograms are found to perfectly match the simulated ones with Fresnel diffraction integral as observed in the third and fourth rows of Fig. 1.

### OAM MODE PURITY MEASUREMENT

The first step in the characterization of SPPs is to verify the purity of the generated OAM modes by different SPPs printed on a glass substrate. The purity is quantified by evaluating an inner product of the incoming OAM field  $E_\ell$ , which is produced by an SPP, and a match filter, which is directly related to the phase function  $\exp(-i\ell_{\text{SLM}}\phi)$ , for several  $\ell_{\text{SLM}}$  values encoded in a hologram of the OAM pattern on the SLM. The inner product is optically measured by a charge-coupled device (CCD) detector at the focal plane of the Fourier transform lens [15]. This process is known in the literature as “modal decomposition,” which extracts the modal content of laser beams and determines various properties of the light such as the Poynting vector of a beam. We recall that SLMs are electrically programmable devices based on liquid crystal molecules, which can spatially alter the phase of

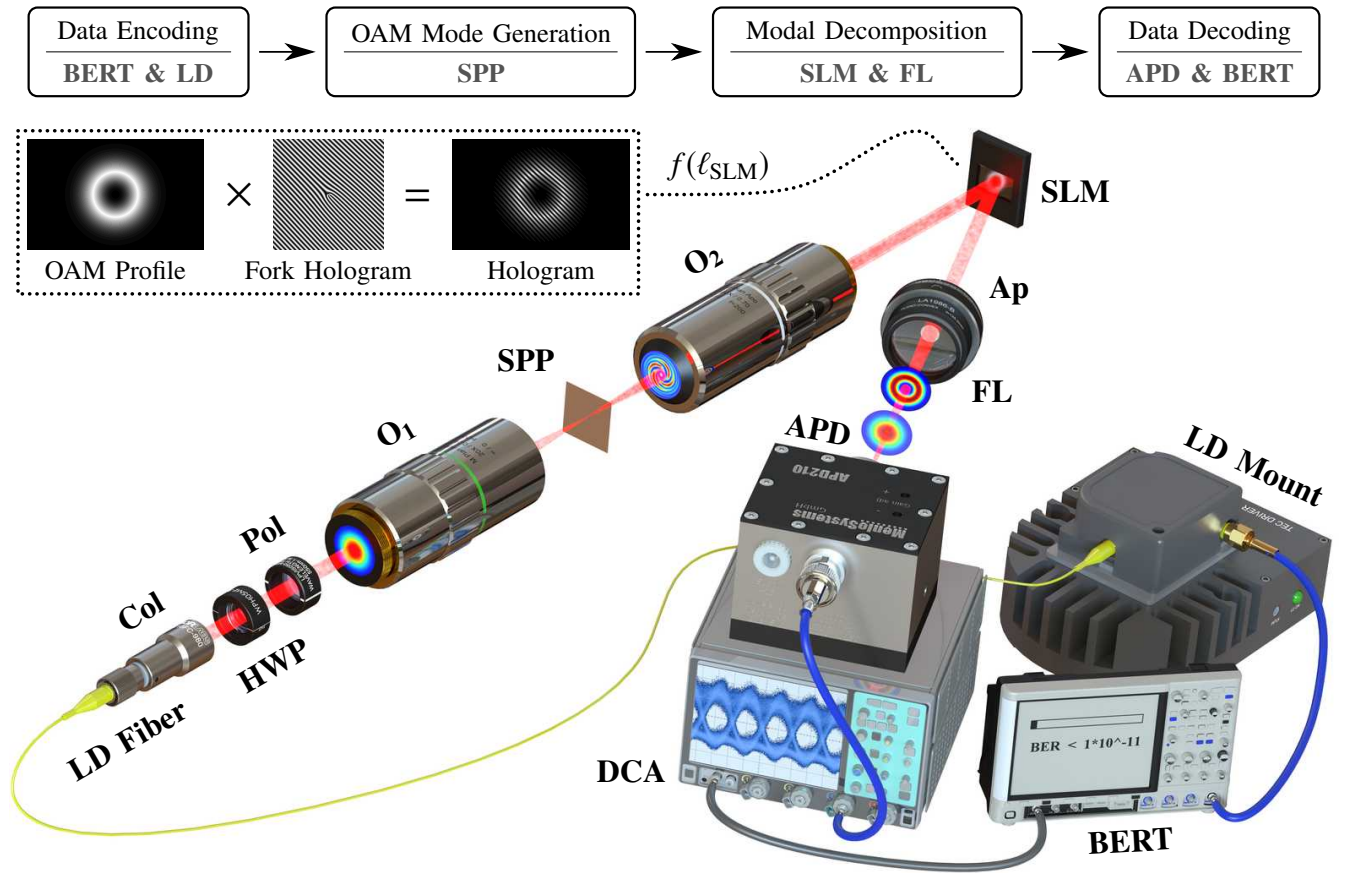


**Figure 2.** Schematic of the experimental setup. LD: laser diode; Col: collimator; HWP: half-wave plate; Pol: polarizer; SPP: spiral phase plate; SLM: spatial light modulator; APD: avalanche photodetector; O<sub>1</sub> and O<sub>2</sub>: 20x/0.42 NA and 50x/0.42 NA objectives, respectively (NA: numerical aperture); Ap: aperture; FL: Fourier lens; DCA: digital communication analyzer; BERT: bit error rate tester.

an incident beam using a computer-generated hologram [15]. The holograms in our measurements are generated using an amplitude modulation technique on a phase-only device [15, references therein]. Only when the match filter corresponds to the reverse topological charge of the input OAM mode does the SLM-converted mode become Gaussian-like (i.e., an intensity pattern with a nonzero center point intensity). Any other match filter will generate another OAM mode with a topological charge of  $\ell' + \ell_{\text{SLM}}$ .

The experimental setup in Fig. 2 is used to perform the OAM mode purity measurement. The liquid crystal SLM has a full HD display resolution ( $1920 \times 1080$ ) with  $8 \mu\text{m}$  pixel pitch, which was calibrated for a full-range  $2\pi$  phase shift at the wavelength of 980 nm. A half-wave plate and a polarizer are used to maximize the intensity and match the polarization of the incident light beam with the SLM working polarization direction, and helical-phase pattern holograms are programmed on the SLM with an azimuthal mode index from -10 to 10. Beam intensity profiles are shown at O<sub>1</sub>, O<sub>2</sub>, and the avalanche photodetector (APD). The laser diode in conjunction with the collimator outputs a Gaussian beam at O<sub>1</sub>, but the pattern at O<sub>2</sub> depends on which SPP is used (for comparison, see Fig. 1); in addition, the pattern at APD depends on the SLM hologram that is a function of azimuthal mode index. The

block diagram in Fig. 2 shows the general workflow process.

SPP label	OAM mode	Diameter
S1	$\ell = +1$	20 $\mu\text{m}$
S2	$\ell = -2$	20 $\mu\text{m}$
S3	$\ell = -3$	20 $\mu\text{m}$
S4	$\ell = +2$	100 $\mu\text{m}$
S5	$\ell = -4$	100 $\mu\text{m}$

**Table 1.** Designation of the characterized SPPs.

The purity of the generated OAM modes is assessed with a CCD beam profiler, fixed at the position of the APD to measure the intensity at a fixed-point symmetry center. Then the result for each hologram is normalized with respect to the Gaussian-like mode for each SPP, as shown in Fig. 3 (with the SPP details listed in Table 1). We observe that the generated modes are of high purity. However, for some SPPs, there is slight crosstalk with the neighboring modes mainly due to small system alignment imperfections. One major benefit of using SPPs is that nearly 100 percent of the incident laser



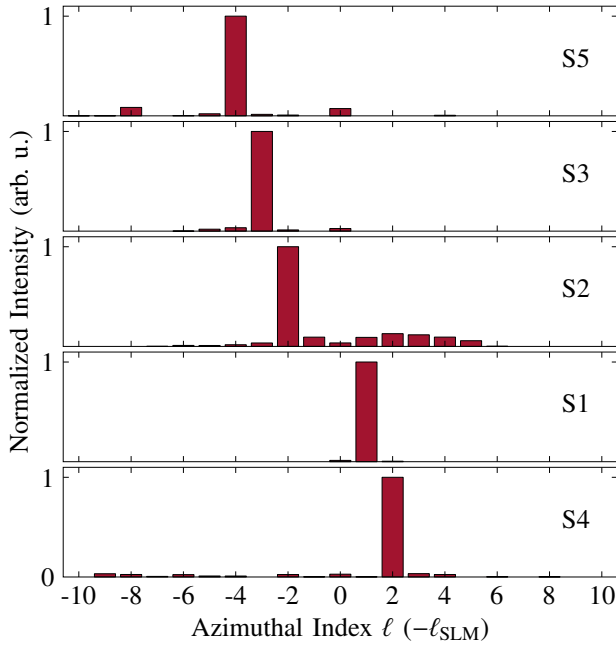


**Figure 3.** OAM mode purity measurements for different SPPs – S1:  $\ell = +1$ ; S2:  $\ell = -2$ ; S3:  $\ell = -3$ ; S4:  $\ell = +2$ ; S5:  $\ell = -4$ .

beam energy is converted into the designated OAM mode, and the conversion process is practically polarization-insensitive, while many state-of-the-art OAM generation techniques suffer from low conversion efficiencies, scattering, and polarization dependence.

### OPTICAL COMMUNICATION PERFORMANCE AND SETUP

To test the potential of using the SPPs in communication systems, we replaced the CCD camera by a high-speed 1-GHz silicon avalanche photodetector synchronized with the laser. A pseudorandom binary sequence non-return-to-zero (NRZ) on-off keying (OOK) data stream generated by a high-performance serial bit error rate (BER) tester was used to modulate the laser and analyze the received signal. Figure 4 shows the eye diagrams obtained by a digital communication analyzer (DCA) at different data rates when SPP S1 was used to produce an OAM mode with a topological charge of +1. The raw data unfiltered eye diagrams are clear for different signal data rates, which reflect high system performance. Our communication system achieved below the detection limit ( $\text{BER} < 10^{-11}$  for the used BER tester) an error-free link up to 1.06 Gb/s and a maximum data rate of 1.80 Gb/s with a BER of  $0.4 \times 10^{-3}$ , which is below the forward error correction (FEC) limit of  $3.8 \times 10^{-3}$ , as shown in Fig. 5. We note that the data rate performance of the system is limited by the APD, since its 3-dB bandwidth falls exactly at 1 GHz. Thus, the fabricated SPPs are not the limiting factor and can produce pure OAM beams to deliver high-bit-rate optical communication channels.

In the case of multiple superimposed OAM beams, when using the intensity modulation direct detection to decode

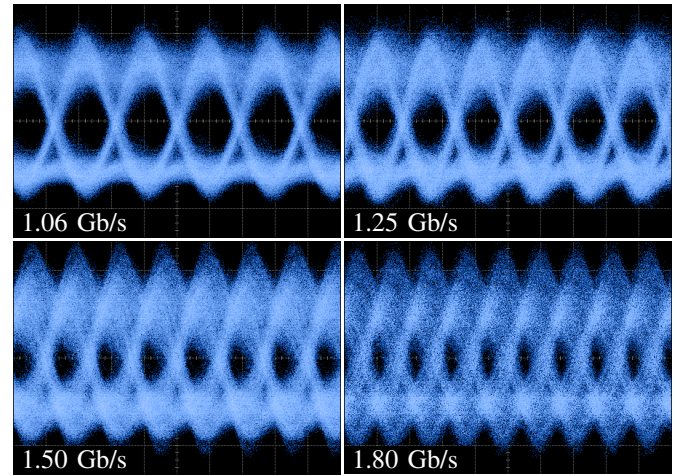


**Figure 4.** Measured eye diagrams for 1.06 Gb/s, 1.25 Gb/s, 1.50 Gb/s, and 1.80 Gb/s data rate signals.

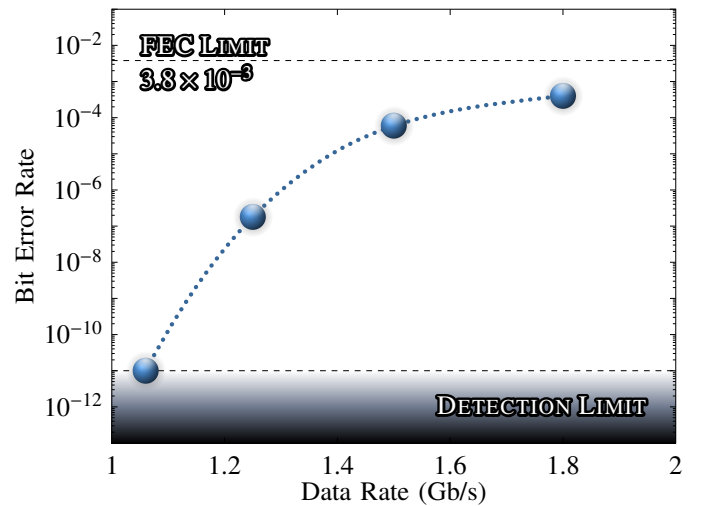


**Figure 5.** Measured BER for 1.06 Gb/s, 1.25 Gb/s, 1.50 Gb/s, and 1.80 Gb/s data rate signals.

a particular signal carried by an OAM beam, we should stress that a spatial separation or filtering is required after demultiplexing. A possible solution to significantly reduce the crosstalk is to couple the Gaussian-like mode into a single-mode fiber connected to an intensity-modulation/direct-detection (IM-DD) receiver or a coherent detector to decode only the information that was initially carried by the transmitted OAM beam.

### CONCLUSION

In conclusion, we have fabricated microscale SPPs that can be used in photonic circuits and realize OAM integrated laser sources. We have verified the SPP OAM modes, measured their purity, and tested the performance of a communication link with one of the fabricated SPPs. We have maintained the high transmission capacity with the minimum BER using a direct modulation-detection scheme. This work paves the way toward cost-effective high-speed OAM-based integrated

free-space communication systems. Microstructured SPPs can further contribute to bringing OAM to the chip level for photonic integrated circuits for numerous applications. OAM light sources based on microscale SPPs will find potential applications in both classical optical communication and quantum information systems.

#### ACKNOWLEDGMENT

The authors acknowledge the funding from King Abdullah University of Science and Technology (KAUST) BAS/1/1614-01-01, KCR/1/2081-01-01, GEN/1/6607-01-01, and BAS/1/1064-01-01.

#### REFERENCES

- [1] M. J. Padgett, "Orbital Angular Momentum 25 Years On," *Opt. Express*, vol. 25, no. 10, May 2017, pp. 11,265–74. [DOI] [↗](#)
- [2] L. Allen *et al.*, "Orbital Angular Momentum of Light and the Transformation of Laguerre-Gaussian Laser Modes," *Phys. Rev. A*, vol. 45, no. 11, June 1992, pp. 8185–89. [DOI] [↗](#)
- [3] A. E. Willner *et al.*, "Optical Communications Using Orbital Angular Momentum Beams," *Adv. Opt. Photon.*, vol. 7, no. 1, Mar. 2015, pp. 66–106. [DOI] [↗](#)
- [4] L. A. Rusch *et al.*, "Carrying Data on the Orbital Angular Momentum of Light," *IEEE Commun. Mag.*, vol. 56, no. 2, Feb. 2018, pp. 219–24. [DOI] [↗](#)
- [5] J. Wang *et al.*, "Terabit Free-Space Data Transmission Employing Orbital Angular Momentum Multiplexing," *Nat. Photonics*, vol. 6, no. 7, June 2012, pp. 488–96. [DOI] [↗](#)
- [6] N. Bozinovic *et al.*, "Terabit-Scale Orbital Angular Momentum Mode Division Multiplexing in Fibers," *Science*, vol. 340, no. 6140, June 2013, pp. 1545–48. [DOI] [↗](#)
- [7] S. Yu, "Potentials and Challenges of Using Orbital Angular Momentum Communications in Optical Interconnects," *Opt. Express*, vol. 23, no. 3, Feb. 2015, pp. 3075–87. [DOI] [↗](#)
- [8] J. Dong *et al.*, "A High Repetition Rate Passively Q-Switched Microchip Laser for Controllable Transverse Laser Modes," *J. Opt.*, vol. 18, no. 5, Mar. 2016, art. no. 055205. [DOI] [↗](#)
- [9] Y. Toda *et al.*, "Single Orbital Angular Mode Emission from Externally Feed-Backed Vertical Cavity Surface Emitting Laser," *Appl. Phys. Lett.*, vol. 111, no. 10, Sept. 2017, art. no. 101,102. [DOI] [↗](#)
- [10] J. Zhang *et al.*, "An InP-Based Vortex Beam Emitter with Monolithically Integrated Laser," *Nat. Commun.*, vol. 9, no. 1, July 2018, art. no. 2652. [DOI] [↗](#)
- [11] Y. Wang *et al.*, "Integrated Photonic Emitter with a Wide Switching Range of Orbital Angular Momentum Modes," *Sci. Rep.*, vol. 6, no. 1, Mar. 2016, art. no. 22512. [DOI] [↗](#)
- [12] Z. Xie *et al.*, "Ultra-Broadband On-Chip Twisted Light Emitter for Optical Communications," *Light Sci. Appl.*, vol. 7, no. 4, Apr. 2018, art. no. 18001. [DOI] [↗](#)
- [13] E. Brasselet *et al.*, "Photopolymerized Microscopic Vortex Beam Generators: Precise Delivery of Optical Orbital Angular Momentum," *Appl. Phys. Lett.*, vol. 97, no. 21, Nov. 2010, art. no. 211108. [DOI] [↗](#)
- [14] T. Gissibl *et al.*, "Refractive Index Measurements of Photorefractive Materials for Three-Dimensional Direct Laser Writing," *Opt. Mater. Express*, vol. 7, no. 7, June 2017, pp. 2293–98. [DOI] [↗](#)
- [15] C. Rosales-Guzman and A. Forbes, *How to Shape Light with Spatial Light Modulators*, vol. SL30, SPIE Press, June 2017. [DOI] [↗](#)

#### BIOGRAPHIES

**EDGARS STEGENBURGS** [S'15] ([edgars.stegenburgs@kaust.edu.sa](mailto:edgars.stegenburgs@kaust.edu.sa)) is a Ph.D. candidate at the Photonics Laboratory, King Abdullah University of Science and Technology (KAUST), Saudi Arabia. He received his M.S. (electrical engineering) from KAUST in 2016 and his B.S. (physics) degree

from the University of Latvia in 2014. Previously, he worked in the Laser Centre of the University of Latvia. His research focuses on the manipulation of light in photonics and optoelectronics. Other research interests include light-matter interaction, numerical analysis, and solid-state lighting applications. He is also a member of OSA and SPIE.

**ANDREA BERTONCINI** [S'19] ([andrea.bertoncini@kaust.edu.sa](mailto:andrea.bertoncini@kaust.edu.sa)) received his M.S. degree in nuclear engineering from Politecnico di Milano, Italy, in 2014. He is currently a Ph.D. candidate at KAUST working on the design and fabrication by direct laser writing 3D printing of micro-optics and photonic structures.

**ABDERRAHMEN TRICHILI** [M'17] ([abderrahmen.trichili@kaust.edu.sa](mailto:abderrahmen.trichili@kaust.edu.sa)) received his diplôme d'ingénieur and Ph.D. degree in information and communication technology from l'École Supérieure des Communications de Tunis (SUP'COM, Tunisia) in 2013 and 2017, respectively. He is currently a postdoctoral fellow in CEMSE at KAUST. His current areas of interest include space-division multiplexing, orbital angular momentum multiplexing, free-space optical communication, and underwater wireless optical communication systems.

**MOHD SHARIZAL ALIAS** [M'08, SM'18] ([mohdsharizal.binalias@kaust.edu.sa](mailto:mohdsharizal.binalias@kaust.edu.sa)) is currently a research associate at the Department of Materials, University of Oxford, United Kingdom. He received his Ph.D. degree (microengineering and nanoelectronics) from the National University of Malaysia in 2010 and his M.S. (physics) and B.S. (physics) degrees from the University of Malaya in 2005 and 2000, respectively. From 2013 to 2018, he was a research scientist at the Photonics Laboratory, KAUST. His research focuses on the usage of nanophotonics to enhance light manipulation for photonic devices. His other research interests include semiconductor lasers and the micro/nanofabrication process.

**TIEN KHEE NG** [M'09, SM'17] ([tienkhee.ng@kaust.edu.sa](mailto:tienkhee.ng@kaust.edu.sa)) received his Ph.D. (2005) and M.Eng. (2001) from Nanyang Technological University (NTU), Singapore. He was a test engineer at Hewlett-Packard Singapore (1997–1998), a member of technical staff with Tinggi Technologies (2004–2006), and a research fellow at NTU until 2009. He is a senior research scientist in Prof. Ooi's group at KAUST. As a coprincipal-investigator responsible for innovation in MBE-grown nanostructures devices in the KACST Technology Innovation Center at KAUST, he realized wide-bandgap nitride quantum-confined and nanowires structures to address efficient light emitters, optical wireless communications, and energy harvesting.

**MOHAMED-SLIM ALOUINI** [S'94, M'98, SM'03, F'09] ([slim.alouini@kaust.edu.sa](mailto:slim.alouini@kaust.edu.sa)) received his Ph.D. degree in electrical engineering from the California Institute of Technology (Caltech), Pasadena, in 1998. He served as a faculty member at the University of Minnesota, Minneapolis, then at Texas A&M University at Qatar, Education City, Doha, before joining KAUST as a professor of electrical engineering in 2009. His current research interests include the modeling, design, and performance analysis of wireless communication systems.

**CARLO LIBERALE** [M'19] ([carlo.liberales@kaust.edu.sa](mailto:carlo.liberales@kaust.edu.sa)) received his M.S. and Ph.D. degrees from Pavia University, Italy, in 2000 and 2004, respectively. His research interests focus on developing and applying label-free chemical imaging techniques based on vibrational spectroscopy (infrared and Raman microspectroscopy) and multiphoton processes (coherent Raman microscopy, second-harmonic generation). One of the main goals of this research activity is to unveil specific biochemical signatures of cancer stem cells with a particular focus on understanding the dysregulation of their lipid metabolism. He is also interested in using high-resolution 3D printing based on direct laser writing to fabricate novel micro-optics toward the miniaturization of complex optical systems and smart micro/nanostructures for use as a probe in nanoscale imaging.

**BOON S. OOI** [M'95, SM'03] ([boon.ooi@kaust.edu.sa](mailto:boon.ooi@kaust.edu.sa)) is a professor of electrical engineering at KAUST. He received a Ph.D. degree from the University of Glasgow, United Kingdom, in 1994. He joined KAUST from Lehigh University in 2009. His recent research is concerned with the study of III-nitride-based materials and devices and lasers for applications such as solid-state lighting, visible-light and underwater wireless optical communications, and energy-harvesting devices. He has served on the Technical Program Committees of CLEO, IPC, ISLC, and IEDM. He currently serves on the Editorial Boards of Optics Express and the IEEE Photonics Journal. He is a Fellow of OSA, SPIE, and IoP.